SUPERCONDUCTING MAGNETIC ENERGY STORAGE SYSTEMS

H. Brechna, F. Arendt and W. Heinz
Institut für Experimentelle Kernphysik
Kernforschungszentrum Karlsruhe, W. Germany

Abstract

Magnetic energy storage systems capable of storing energies in the order of 10^{10} J or higher will be required within the next decade to provide the magnetic fields in thermonuclear fusion reactors. In this paper, various aspects for pulsed and steady state magnetic storage systems capable of providing the energies mentioned are discussed. The coil size and maximum central field in the magnet system are limited by the magnetomechanical forces, which require special high strength stabilized conductors and appropriate coil reinforcements. Problems of safety, shielding of electromagnetic fields, switching, thermal losses, and economical considerationsare presented.

I. Introduction

Energy that may easily be reconverted into useful electric energy may be stored in a number of ways: as electric charge in a capacitor, as inductive energy in a magnet, as chemical energy in accumulators, as kinetic energy in mechanical systems, and as potential energy in pumpstations. Storage units of this type in the range of MJ are needed in several areas of physics and engineering, particularly in solid state physics, high energy physics, plasma physics, and in controlled thermonuclear reactors. Possible further applications are for peak shaving and storage of energy in electrical power grids. Since the storage and extraction systems have to be adapted to the particular application, it is not possible to generalize the most preferable method of storage.

Capacitors are discharged efficiently in a time up to 100 μsec and have a low energy density of ~ 0.2 J/cm^3.

Rotating machines and batteries are used for slow energy extraction in the range of seconds and above; they have an energy density in the order of about 200 J/cm^3. A battery delivers its maximum power if the resistancesof load and cell are equal. In this case, half the energy is dissipated in the cell, and the energy efficiency is 50%. Depending on the time of energy extraction, the efficiency varies between $\sim 5\%$ for fast extraction ($\lesssim 1$ sec) and more than 90% for slow extraction over several hours.

In a superconducting inductive energy storage, maximum fields of about 15 T may reasonably be generated, giving an energy density of 90 J/cm^3. At energies above $\sim 10^7$ J, these storage units are most economical compared to other means of energy storage for discharge times in the range of 10^{-3} - 10 sec. The minimum discharge time depends on the time constant of the discharge circuit. For good power efficiency, the current should not flow from the storage to the load in times approaching the field decaytime constant. In Fig. 1 we have illustrated means of energy storage and the time range of their efficient energy discharge[1] which may also be considered as their range of usefulness. The curve for inductive storage units is based on a current of 10^6 A assuming that the switch for such currents is available.

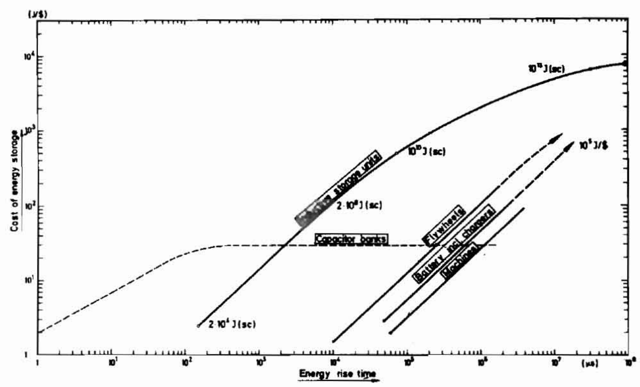

Fig. 1 Cost of energy storage vs energy rise time.

The generation of pulsed magnetic fields requires energy sources of high power. The existing electric networks are not capable of delivering the power within the required time and thus, an intermediate energy storage device is needed. Superconducting storage systems may act as a compensating link between pulsed loads as proposed by Smith[2] for synchrotrons where high quality factors are required.

Storage of energy in the multi-megajoule range is needed for fusion experiments where 3 types of plasma-devices are currently in use:

i) stationary machines with external dc-field coils (e.g. stellerators),
ii) quasi-stationary or slowly pulsed machines (e.g. tokamaks) with a coil for the azimuthal main field and a transformer to provide an inductive current in the plasma which produces the necessary meridional field,
iii) fast pulsed machines (e.g. Θ-pinch).

The economy of fusion reactors depends on essentially three items: the plasma confining magnet system, the plasma heating system and the energy storage system. The cost of a superconducting magnet system for a toroidal fusion reactor is about $ 25 - $ 100 per kW_e[3,4] depending on the complexity of the magnet system, the optimism concerning the price of the composite conductor, and the overall designs of the reactor. The cost of the magnet-system is in the range of 1/2 to 2/3 of the reactor! Today, the specific cost for a conventional or nuclear power plant of several hundred MW is about $ 150 per kW.

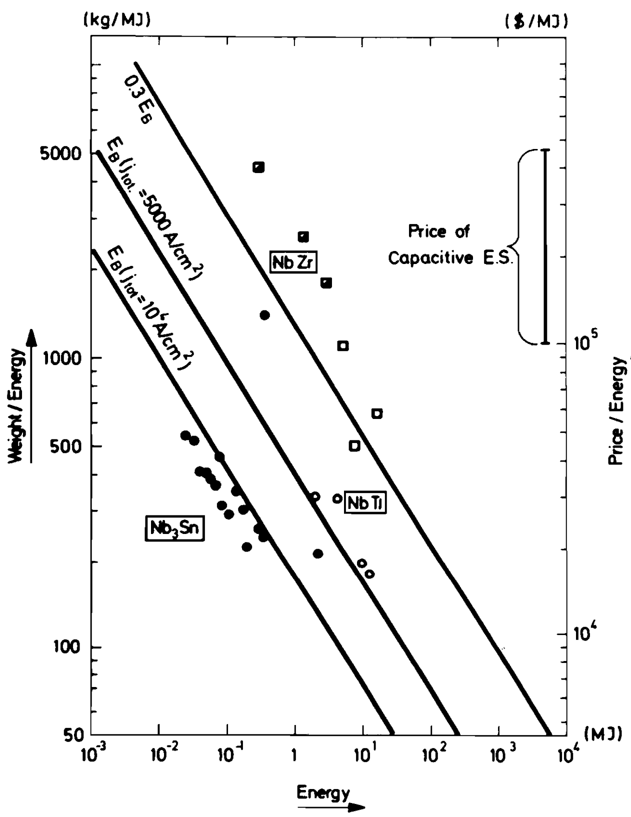

Fig. 2 Cost and weight of superconducting coils vs energy (Stekly 1970).

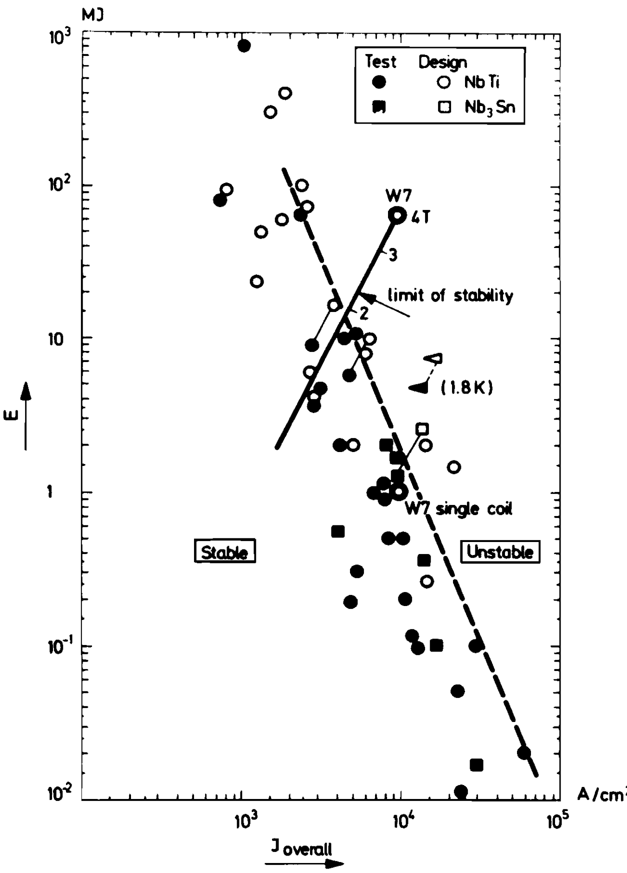

Fig. 3 Review of stored energy in coils already built vs overall current density (Lubell, Wipf).

Inductive energy storage units for peak power shaving and the replacement of energy pumpstations will be technically feasible but economically about a factor of 10 more expensive than conventional energy storage systems. However, with the present trend this factor may shift in favor of superconducting devices.

Based on the superconductor utilized for energy storage, Fig. 2 illustrates the cost and weight of energy storage units as a function of the stored energy. As a comparison, capacitive storage units are shown. For large units, the choice of current density depends on the forces, which determine the maximum values. However, application of new methods of reinforcements may yield current densities in the order of 1000 Acm^{-2} for units in the range of 10^{10} J. Depending on the choice of the superconductor, the stability criterion limits the maximum current density as a function of energy. Lubell[5] has compiled the magnets built to date, which illustrate

$ 10⁴/MJ @ 10³ MJ

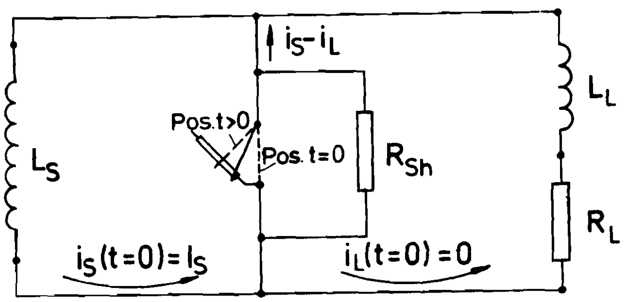

a

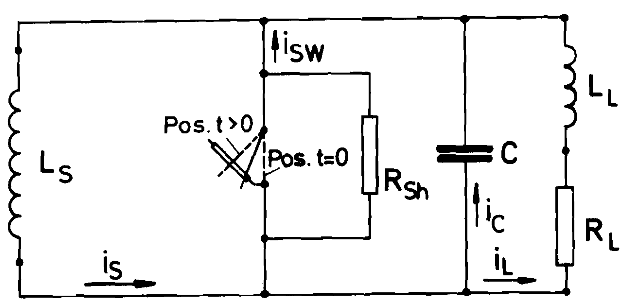

b

Fig. 4 Energy storage and load circuit. The superconducting switch is represented by a variable resistor.

the trend where most coils are placed. Only few magnets have exhibited a marked improvement as compared to the usual magnets (Fig. 3).

II. Energy Transmission

With the assumption that an inductive energy storage unit is discharged over a switch into an inductive load (Fig. 4), the circuit equations are written in the usual form for time independent R_L.

$$L_S \frac{di_S}{dt} + R_{SW}\,(i_S - i_L) = 0 \qquad (1)$$

$$L_L \frac{di_L}{dt} + R_{SW}\,(i_L - i_S) + i_L\,R_L = 0. \qquad (2)$$

By putting $A = L_L/L_S$ and $B = R_L/R_{SW}$ and using the boundary conditions $i_S(t = 0) = I_S$, $i_S(t = \infty) = 0$, $i_L(t = 0) = 0$ and $i_L(t = \infty) = 0$ we obtain:

$$i_S(t) = \frac{I_S}{\delta-\gamma}\left[(1-\gamma)\cdot\exp\left(\frac{-t}{\tau_2}\right) - (1-\delta)\cdot\exp\left(\frac{-t}{\tau_3}\right)\right], \qquad (3)$$

$$i_L(t) = I_S\cdot\frac{(1-\gamma)(1-\delta)}{(\delta-\gamma)}\left[\exp\left(\frac{-t}{\tau_2}\right) - \exp\left(\frac{-t}{\tau_3}\right)\right] \qquad (4)$$

with $\gamma = \frac{0.5}{A}\left[1+A+B - ((A-B)^2+2A+2B+1)^{1/2}\right]$

$$\delta = \frac{0.5}{A}\left[1+A+B + ((A-B)^2+2A+2B+1)^{1/2}\right],$$

$$\tau_2 = \frac{L_S}{\delta\cdot R_{SW}} \quad \text{and} \quad \tau_3 = \frac{L_S}{\gamma\cdot R_{SW}}\ .$$

The voltage across the load is given by:

$$U_L(t) = \frac{R_{SW}\cdot I_S}{\delta-\gamma}\left[\left(\frac{B}{A}-\gamma\right)\exp\left(\frac{-t}{\tau_3}\right)-\left(\frac{B}{A}-\delta\right)\exp\left(\frac{-t}{\tau_2}\right)\right]$$

It can be seen that for A = 1 this voltage is nearly independent of B for values up to 10.

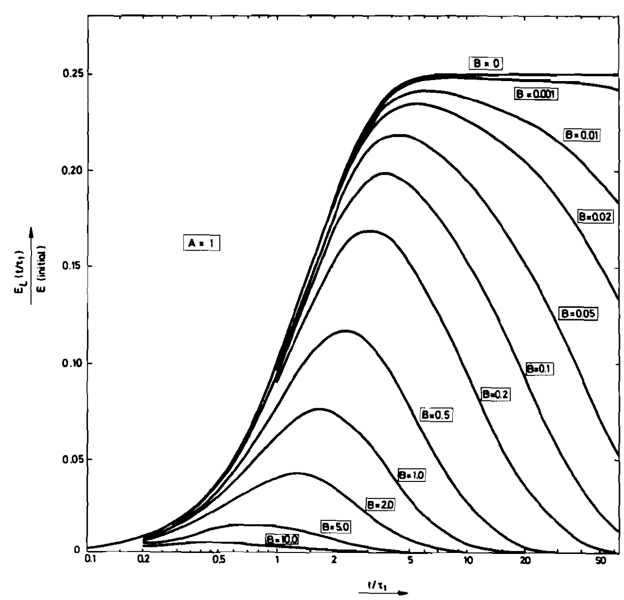

Fig. 5 Energy transmitted to the load with load resistance R_L as parameter ($\tau_1 = L_S/2R_{SW}$).

In these equations, R_{SW} represents the resistance of the switch including the shunt resistance R_{Sh}.

The energy transmission from the storage unit to the load with R_L as a parameter and A = 1 is illustrated in Fig. 5. The peak energy transmitted to the load occurs at A = 1 and $R_L = 0$. For $R_L = 0$, the initial stored energy is $E_S(t = 0) = 0.5 \times L_S I_S^2$, the final energy in the load $0.25 \times E_S(t = 0)$ and the final energy in the storage $E_S(t = \infty) = 0.25 \cdot E_S(t = 0)$. The energy dissipated in the switch is $0.5 \cdot E_S(t = 0)$. These conditions are shown in Fig. 6. Thus, for $R_L = 0$, only 25% of the initial stored energy is transmitted into the load.

We consider two cases:

i) B = 0;

with: $\gamma = 0, \quad \delta = \frac{1+A}{A}$.

We obtain: $i_S(t = 0) = I_S$

$$i_S(t = \infty) = I_S \frac{1}{1+A}$$

$$i_L(t = \infty) = I_S \frac{1}{1+A}$$

and $$E_S(\text{final}) = E_S(\text{initial}) \frac{1}{(1+A)^2}$$

$$E_L(\text{final}) = E_S(\text{initial}) \frac{A}{(1+A)^2}$$

$$E_{SW}(\text{lost}) = E_S(\text{initial}) \frac{A}{1+A}$$

ii) $R_L/R_{SW} = B \neq 0$

$$E_L(\text{lost}) = E_S(\text{initial}) \frac{1}{1+A+B}$$

The energy loss in the switch is given by:

$$E_{SW}(\text{lost}) = E_S(\text{initial}) \frac{A+B}{1+A+B}$$

The transfer of energy is improved if a capacitor is used as a transfer impedence. To compare the energy transferred to the case illustrated in Fig. 6 (top), we assume that the circuit breaker is opened at t = 0 and the current i_S flows through L_S. Ignoring R_L we have the well-known equation:

$$L_S \frac{d^2 i_S}{dt^2} + \frac{i_S - i_L}{C} = 0 \qquad (5)$$

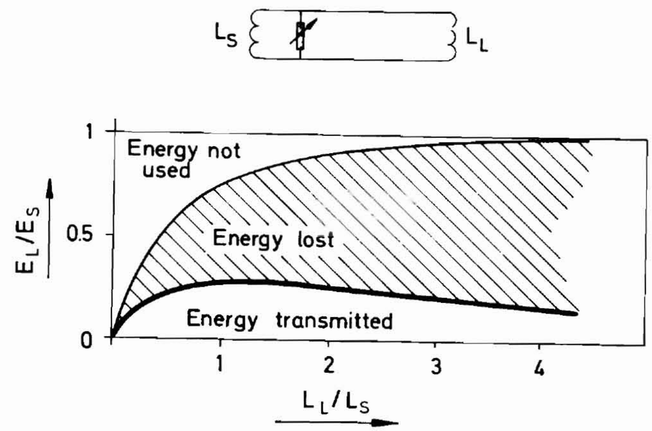

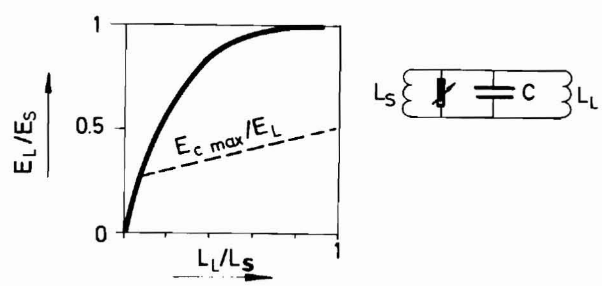

Fig. 6 Ratio of transmitted energy to the stored energy vs ratio of inductances L_L/L_S. If a capacitor is used as transfer impedance, for $L_L/L_S = 1$ all the stored energy in L_S can be transmitted to the load.

$$L_L \frac{d^2 i_L}{dt^2} - \frac{i_S - i_L}{C} = 0 \qquad (6)$$

which yields:

$$\frac{d^4 i_L}{dt^4} + \left(\frac{L_S + L_L}{L_S L_L C}\right) \frac{d^2 i_L}{dt^2} = 0 \qquad (7)$$

Since at t = 0, $i_S = I_S$ and $i_L = 0$, $di_S/dt = 0$; $di_L/dt = 0$, we have:

$$i_L = I_S \frac{L_S}{L_L + L_S} [1 - \cos(\omega t)] \qquad (8)$$

with the maximum value of

$$i_{L,max} = 2I_S \cdot \left(\frac{L_S}{L_L+L_S}\right) .$$

The proportion of the maximum energy in the load to the energy initially stored, is given by

$$\frac{E_L(\max)}{E_S(\text{initial})} = 4 \cdot \frac{L_L/L_S}{(1+L_L/L_S)^2} \qquad (9)$$

If $L_L = L_S$: $\frac{E_L(\max)}{E_S(\text{initial})} = 1$,
as shown in Fig. 6 bottom.

The voltage across the capacitor is given by:

$$U_C = \frac{1}{C}\int(i_S - i_L)\,dt = \frac{I_S}{\omega C}\sin(\omega t) \qquad (10)$$

which has a peak value of $\frac{I_S}{C} \cdot \sqrt{\frac{L_S L_L C}{L_S+L_L}}$;

or if $L_S = L_L$: $U_{max} = I_S \cdot \sqrt{\frac{L_S}{2C}}$.

The required energy storage capability of the capacitor is given by:

$$\frac{E_C}{E_S(\text{initial})} = \frac{L_L}{L_L+L_S} \qquad (11)$$

If the inductances are equal the capacitance must be capable of storing half the energy of the inductive storage unit.

III. Circuit Arrangements

Schematic circuit arrangements with a storage coil L_S, an inductive load L_L, a resistive load R_L and a transfer element SW are shown in Fig. 7.

The storage and the transfer element are enclosed in a cryogenic environment (dashed line). The transfer element can be a variable resistance or a variable inductance. In the first case, energy loss is encountered, while in the case of the inductive transfer element mechanical displacements are required.

A normal going superconductor as a switch was proposed by Mawardi.[6] In order to prevent an energy loss in the "normal" superconductor, a shunt resistor R_{Sh} is provided, which is generally not cooled to cryogenic temperature. Further refinement of the energy transfer circuits shown in Fig. 7 (top) is achieved by using a

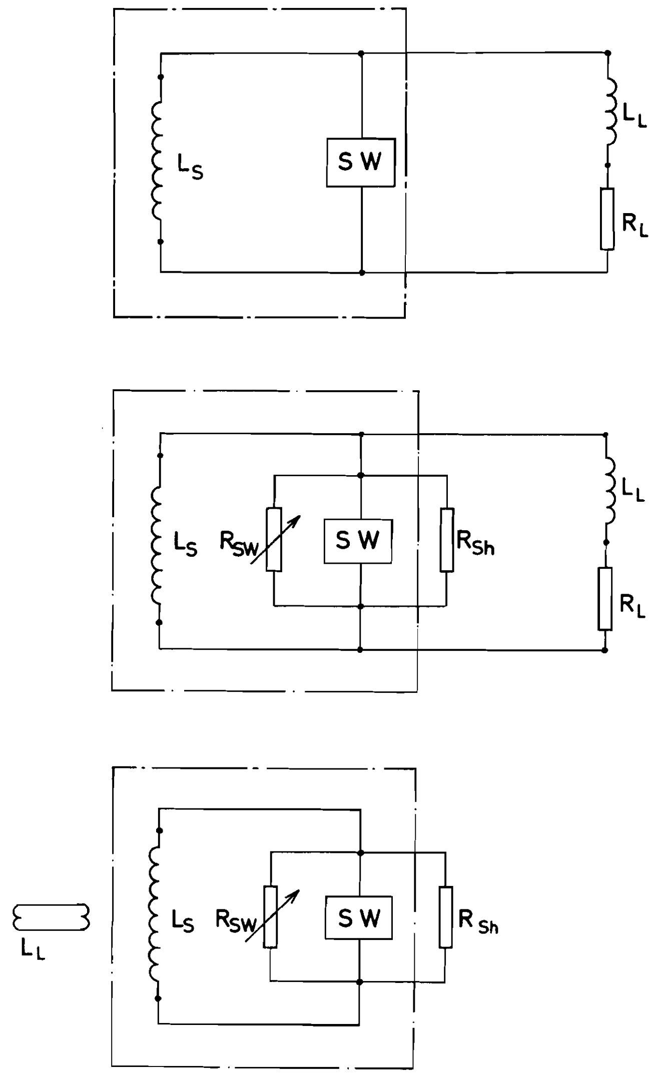

Fig. 7 Arrangements of storage coil L_S, load L_L and a energy transfer element SW.

voltage step down transformer, with the load being connected to its secondary side. The protective shunt R_{Sh} is only effective if $R_{SW} >> R_{Sh}$ and if the transition time constant τ_{SW} is considerably shorter than the transfer time constant τ_{tr}, otherwise the energy dissipation in the switch would be large. Hake[7] has shown that since the switch must carry a current near J_c before switching and must have a normal resistivity ρ_{SW} after switching, its minimum volume V_{SW} is determined by E_S and by τ_{tr} as:

$$V = 2a\, E_S/\tau_{tr} \cdot J_c^{\,2} \cdot \rho_{SW} \qquad (12)$$

where $a = R_{SW}/R_{Sh} \gg 1$. For $J_c \sim 10^5$ A/cm^{-2} and $\rho_{SW} \sim 10^{-4}$ Ωcm, the enthalpy of the switch is sufficiently high to prevent switch burnout. NbTi filaments embedded in CuNi matrix were found to comply with these requirements. However, burnout will be of real concern if $J_c > 3 \times 10^5$ Acm^{-2} and low melting superconductors are used.[8]

Even if the efficiency of the inductive coil is about 20 - 25%, the cost of the storage units in fusion reactors will be less (Fig. 1) than that of capacitor banks. Cryogenic magnetic energy storage and switching units are necessary to make large scale plasma experiments economically feasible.

IV. High Field Coils as a Mean of Energy Storage

The possibility to store energies in superconducting coils with densities of ≥ 50 MJ/m^3 has intensified the study of coil configurations for energy storage.

While studying superconducting coils, two major problems have to be considered: The magnetomechanical forces (Lorentz forces) which limit the peak overall current density and the static and dynamic losses at low temperatures.

We discuss the design problems for three types of magnets:

i) Solenoids. In Table I, well known equations for solenoids with rectangular cross section and uniform current density distributions are compiled. The geometry factor Λ is obtained from Fig. 8.[9] The special configuration with α = 2, and β = 0.5 generally referred to as "Brooks" coils, has the highest energy density as a function of the superconductor quantity Q_{SC} expressed in Am.

The major advantage of these solenoids is the simplicity of retaining Lorentz forces and a possible coil optimization by subdivision of the coil in a number of coaxial coil section with variable current densities. The major disadvantage is the stray flux which must be shielded from the environment. Thus, a second solenoid with opposite field is required as a shield. The support of the electromagnetic forces between the two coils is a major problem.

ii) Spherical Coils. A possible design of a spherical energy storage is illustrated in Fig. 9. The main coil (1) consists of a number of coaxial solenoids with a cross section approximating a sin(0) distribution. The main coil is surrounded by a field screening coil (2) with opposite currents such that the stray flux is effectively screened. The superconductor is

TABLE I.

Energy stored in solenoids

Solenoid

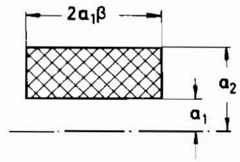

$$L = \Lambda a_1 N^2$$

$$E = 2\Lambda a_1^5 (\lambda J)^2 (\alpha - 1)^2 \beta^2$$

$$V_c = 2\pi a_1^3 (\alpha^2 - 1)\beta$$

$$NI = 2a^2 (\alpha - 1)\beta(\lambda J)$$

$$E = \frac{\Lambda}{2^{2/3}\pi^{5/3}} (\lambda J)^2 \left[\frac{\beta}{(\alpha-1)^2(\alpha+1)^5}\right]^{1/3} V_c^{5/3}$$

$$B(0,0,0) = G\,\frac{NI}{a_1}\left[\frac{\pi(\alpha+1)}{2\beta(\alpha-1)}\right]^{1/2}$$

Brooks Coil

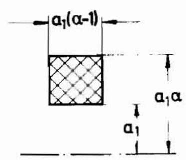

$$\alpha = 2$$

$$L = 25.485 \times 10^{-7} a_1 N^2 \quad \text{(Hy)}$$

$$E = 3.03 \times 10^{-8} V^{5/3} (\lambda J)^2 \quad \text{(J)}$$

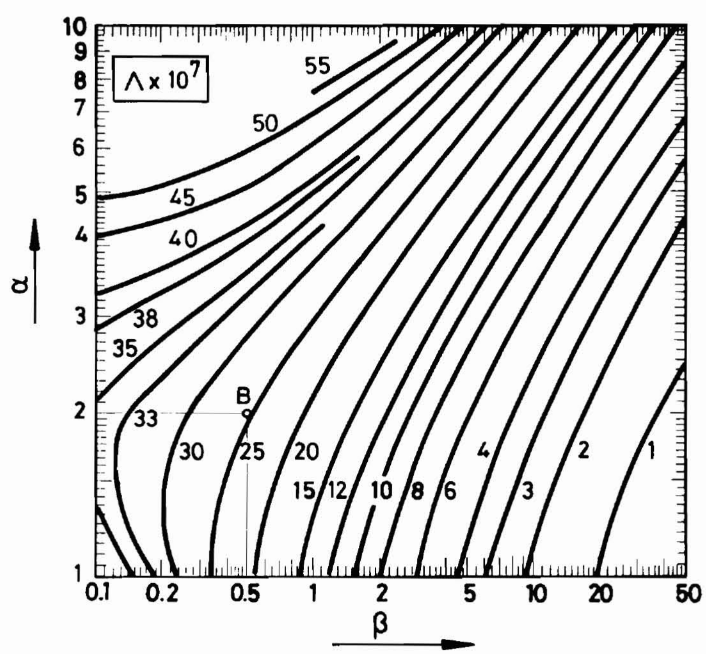

Fig. 8 Inductance factor Λ vs parameters α and β for solenoids. The Λ values for the Brooks coil is indicated for α = 2, β = 0.5.

TABLE II.

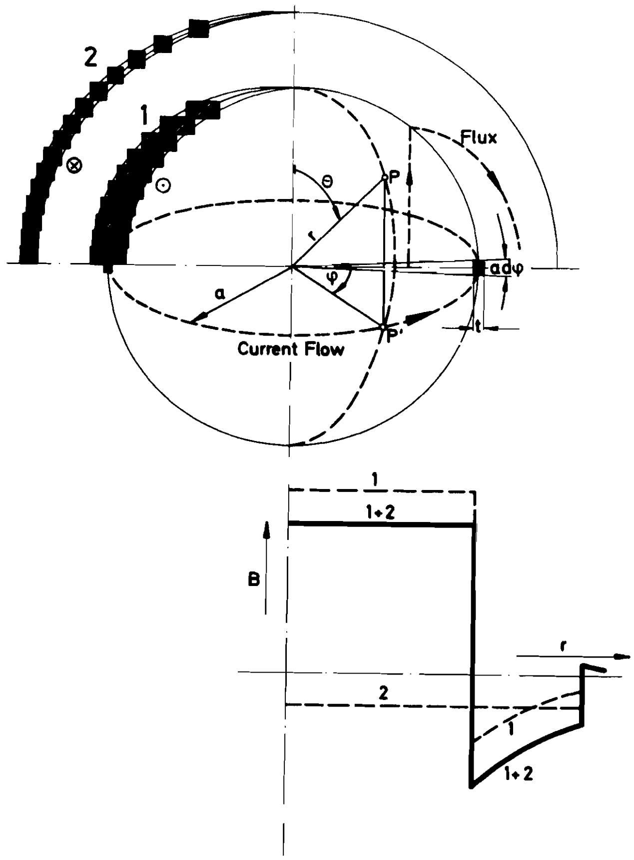

Fig. 9 Spherical energy storage coils. (1) Main Coil (2) Screening Coil. The field distribution is given in the bottom.

Energy stored in spherical coils

Thin wall sphere

$$NI = 2a_1^2(\alpha-1)(\lambda J_0)$$

$r < a_1$

$$B_r(r,\Theta) = \frac{2}{3}\mu_0 a_1(\alpha-1)(\lambda J_0)\cos\Theta$$

$$B_\Theta(r,\Theta) = -\frac{2}{3}\mu_0 a_1(\alpha-1)(\lambda J_0)\sin\Theta$$

$r > a_1$

$$B_r(r,\Theta) = \frac{2}{3}\mu_0\left(\frac{a_1}{r}\right)^3 a_1(\alpha-1)(\lambda J_0)\cos\Theta$$

$$B_\Theta(r,\Theta) = \frac{1}{3}\mu_0\left(\frac{a_1}{r}\right)^3 a_1(\alpha-1)(\lambda J_0)\sin\Theta$$

$$E_{tot} = \frac{4\pi}{9}\mu_0 a_1^5(\alpha-1)^2(\lambda J_0)^2$$

$$E_{tot} = \frac{1}{3\left(\frac{4\pi}{3}\right)^{2/3}}\mu_0\cdot\frac{(\alpha-1)^2}{(\alpha^3-1)^{5/3}}(\lambda J_0)^2 V^{5/3}$$

$$Q_{SC} = \pi^2 a_1^3(\alpha-1)(\lambda J_0)$$

$$E_{tot} = \frac{4}{9\pi^3}\mu_0\frac{Q_{SC}^2}{a_1}$$

Thick wall sphere

$$NI = a_1^2(\alpha^2-1)(\lambda J_0)$$

$r < a_1$

$$B_r(r,\Theta) = \frac{2}{3}\mu_0 a_1(\alpha-1)(\lambda J_0)\cos\Theta$$

$$B_\Theta(r,\Theta) = -\frac{2}{3}\mu_0 a_1(\alpha-1)(\lambda J_0)\sin\Theta$$

$r > a_2$

$$B_r(r,\Theta) = \frac{\mu_0}{6}a_1(\alpha^4-1)(\lambda J_0)\left(\frac{a_1}{r}\right)^3\cos\Theta$$

$$B_\Theta(r,\Theta) = \frac{\mu_0}{12}a_1(\alpha^4-1)(\lambda J_0)\left(\frac{a_1}{r}\right)^3\sin\Theta$$

$a_1 \leq r \leq a_2$

$$B_r(r,\Theta) = \frac{2}{3}\mu_0\left[a_1\left[\alpha-2\left(\frac{a_1}{2r}\right)^3\right]-\frac{3}{4}r\right](\lambda J_0)\cos\Theta$$

$$B_\Theta(r,\Theta) = \frac{2}{3}\mu_0\left[\frac{9}{8}r-a_1\left(\frac{a_1}{2r}\right)^3-a_1\alpha\right](\lambda J_0)\sin\Theta$$

$$E_{tot} = \frac{2\pi}{45}\mu_0 a_1^5(\lambda J_0)^2 f(\alpha)$$

$$E_{tot} = \frac{\mu_0}{30\left(\frac{4\pi}{3}\right)^{2/3}}(\lambda J_0)^2 V^{5/3} g(\alpha)$$

$$Q_{SC} = \frac{\pi^2}{3}(\lambda J_0)a_1^3(\alpha-1)(\alpha^2+\alpha+1)$$

$$E_{tot} = \frac{2\mu_0}{5\pi^3}\cdot\frac{Q_{SC}^2}{a_1}h(\alpha)$$

$$f(\alpha) = (\alpha-1)^2(\alpha^3+2\alpha^2+3\alpha+4)$$

$$g(\alpha) = \frac{(\alpha-1)^2(\alpha^3+2\alpha^2+3\alpha+4)}{(\alpha^3-1)^{5/3}}$$

$$h(\alpha) = \frac{\alpha^3+2\alpha^2+3\alpha+4}{(\alpha^2+\alpha+1)^2}$$

optimally utilized if the ratio of the two coil radii is 1.59 and the ratio of current densities 0.25.[10] Table II gives most pertinent data for a thin shere with $\alpha = a_2/a_1 \approx 1$ and for thick wall spheres with $\alpha > 1$. The calculation is based on a sin(Θ) current density distribution which will also approximate a coil of uniform current density but sin(Θ) cross sectional distribution. To optimize the amount of superconductor, the quantity $Q_{SC} = \int_{Vol}(\lambda J)\,dV$ has been calculated.

iii) Toroidal Coils. The toroidal coil studied is shown in Table III, where design equations and the stored energy are given for coils with constant current density distribution. Since the field within the bore is maximum at P, the current density in the superconductor must be matched to this field. However, current density optimization is recommended in form of concentric toroidal coils similar to the method used in solenoids.

Parametric curves of the stored energy are given in Fig. 10, 11 and 12 to optimize the coil volume or Q_{SC}.

V. Electromagnetic Forces

Since the electromagnetic forces acting on the coils in form of radial outward bursting forces and compressive forces limit the current density in the coil and with it the energy density, their knowledge and restrain becomes one of the main problems in designing large storage units. Both hoop and compressive forces are proportional to the body forces:

$$F_r = B_\Theta J \qquad (N/m^3)$$

$$F_\Theta = B_r J \qquad (N/m^3)$$

TABLE III.

Energy stored in toroidal coils

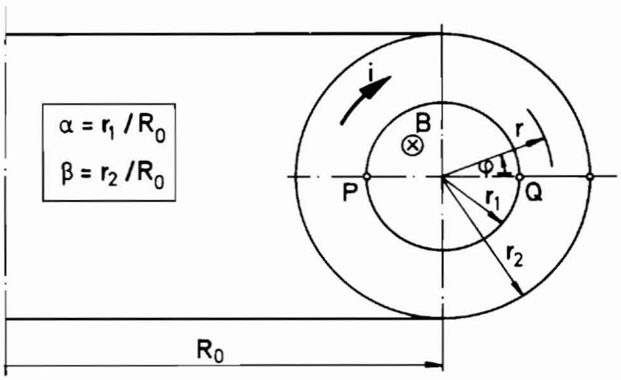

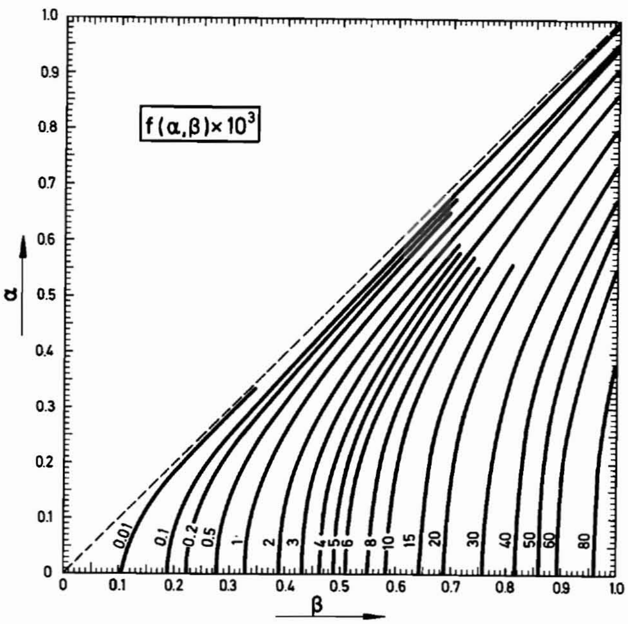

Fig. 10 Geometry factor f(α,β) for the energy stored in a toroid in dependence on the large radius and the overall current density.

$$NI = 2\pi(\lambda J)\cdot R_0(r_2 - r_1) \qquad r_1 < r < r_2$$

$$NI = 2\pi(\lambda J)\cdot R_0(r_2 - r) \qquad r < r_1$$

$$B = \frac{\mu_0}{2\pi}\cdot\frac{NI}{R_0 + r\cos\varphi}$$

$$B_{max} = \frac{\mu_0}{2\pi}\cdot\frac{NI}{R_0 - r_1} = \mu_0(\lambda J)\cdot R_0\,\frac{\beta-\alpha}{1-\alpha}$$

$$V_{tor} = 2\pi^2(\beta^2 - \alpha^2)R_0^3$$

$$Q_{SC} = (\lambda J)V_{tor} = 2\pi^2\frac{B_{max}}{\mu_0}(1-\alpha)(\beta-\alpha)R_0^2$$

$$E_{tot} = 2\mu_0\pi^2 R_0^5(\lambda J)^2\cdot f(\alpha,\beta)$$

$$E_{tot} = \frac{\mu_0}{(2\pi^2)^{2/3}}\cdot V_{tor}^{5/3}(\lambda J)^2\cdot g(\alpha,\beta)$$

$$E_{tot} = \frac{\mu_0}{2\pi^2}\cdot\frac{(Q_{SC})^2}{R_0}\cdot h(\alpha,\beta)$$

$$f(\alpha,\beta) = (\beta-\alpha)^2\left[1-(1-\alpha^2)^{1/2}\right] + \beta(\beta-\alpha)(1-\alpha^2)^{1/2} + \beta\left[\sin^{-1}(\alpha) - \sin^{-1}(\beta)\right] + (1-\alpha^2)^{1/2} - (1-\beta^2)^{1/2} + \frac{1}{3}\left[(1-\beta^2)^{3/2} - (1-\alpha^2)^{3/2}\right]$$

$$g(\alpha,\beta) = \frac{f(\alpha,\beta)}{(\beta^2-\alpha^2)^{5/3}} \quad ; \quad h(\alpha,\beta) = \frac{f(\alpha,\beta)}{(\beta^2-\alpha^2)^2}$$

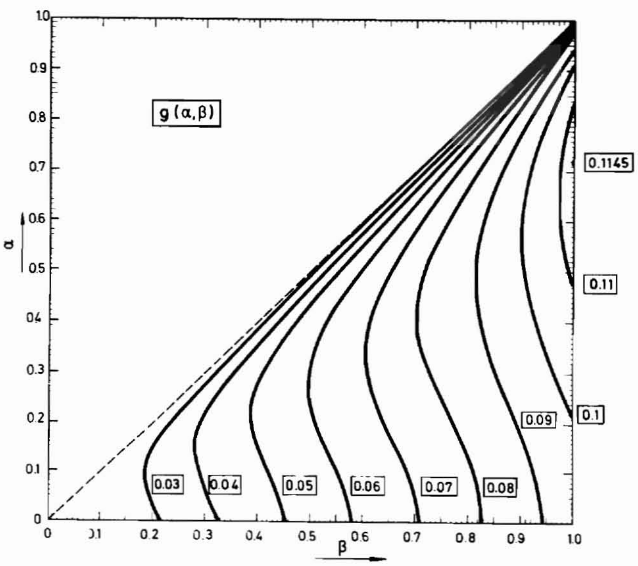

Fig. 11 Geometry factor g(α,β) for the energy stored in a toroid in dependence on the coil volume and the overall current density.

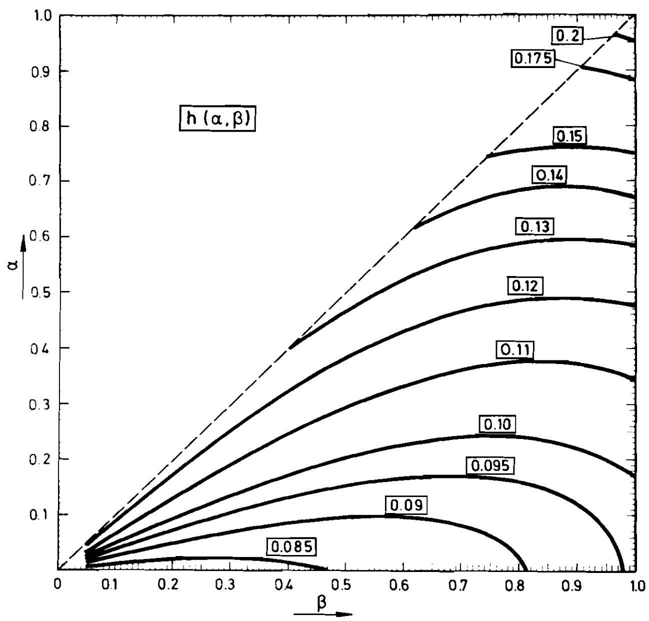

Fig. 12 Geometry factor $h(\alpha,\beta)$ for the energy stored in a toroid in dependence on the large radius and the amount of superconductor used.

In solenoids, B_Θ and F_Θ have to be replaced by B_z and F_z. Calculation of forces in solenoids is familiar.[11] Stress-strain and deformation equations are given for solenoids both in exact form using computational methods and in approximate form. As first order approximation, the circumferential stresses derived by Appleton[12] et al. for solenoids without constraining rings are quite useful:

$$\sigma_\Theta = a_1 \lambda J_o \frac{B_{a1}(\alpha^2+\alpha-2)+B_{a2}(2\alpha^2-\alpha-1)}{6\,\frac{r}{a_1}\,\ln\alpha} \qquad (13)$$

The maximum stress occurs at $r = a_1$, the inner coil radius.

For current optimization solenoids are often subdivided into concentric sections. However, below $\alpha = 2.2$ the regionalization of solenoids increases the maximum stress. For sections with small values of α, stress reduction can be accomplished by support cylinders to carry the stresses. Using high tensile strength materials as a support structure, stresses on the conductor can be reduced by about 20%.

Forces in spherical coils are calculated generally for uniform internal or external pressure and are applicable at the equator only ($\Theta = \pi/2$). The exact evaluation of stresses and deformations in a sphere is quite complex in nature. The equations suitable for computer calculations are given below.

Referring to Fig. 13, the equations relating the stress components and strains for spherical geometries when shear is neglected are:

$$r\,\frac{\partial \sigma_r}{\partial r} + 2\sigma_r - \sigma_\Theta - \sigma_\phi + r\,F_r = 0 \qquad (14)$$

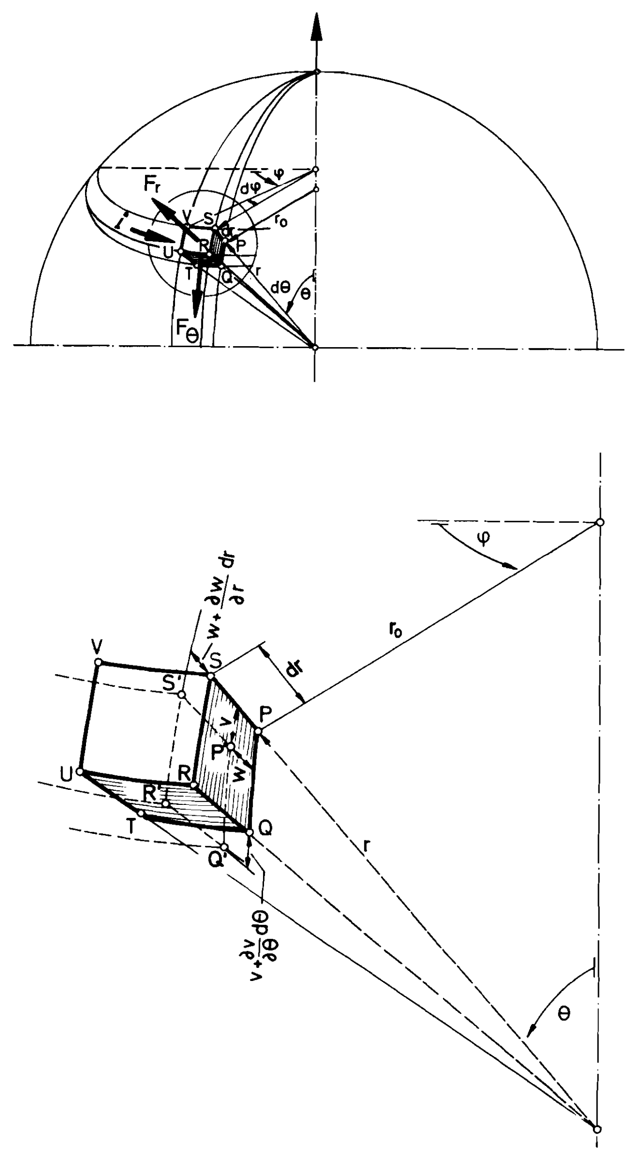

Fig. 13 To calculate stresses in a spherical coil.

$$\sigma_\Theta - \sigma_\phi + \frac{\partial\sigma_\Theta}{\partial\Theta}\tan(\Theta) + r\tan(\Theta)F_\Theta = 0 \quad (15)$$

$$\frac{\partial\sigma_\phi}{\partial\phi} = 0 \quad (16)$$

$$\epsilon_r = \frac{\partial w}{\partial r} = \frac{1}{E}\left[\sigma_r - \nu(\sigma_\phi + \sigma_\Theta)\right] \quad (17)$$

$$\epsilon_\Theta = \frac{1}{r}\left(\frac{\partial v}{\partial\Theta} + w\right) = \frac{1}{E}\left[\sigma_\Theta - \nu(\sigma_r + \sigma_\phi)\right] \quad (18)$$

$$\epsilon_\phi = \frac{1}{r}(v\,\mathrm{cotan}(\Theta) + w) = \frac{1}{E}\left[\sigma_\phi - \nu(\sigma_\Theta + \sigma_r)\right] \quad (19)$$

In these equation, v is the tangential displacement and w the radial displacement of a volume-element.

The body forces are expressed by:

$$F_r = \mu_o(\lambda J_o)^2\left[-\frac{a_1^4}{12r^2} - \frac{2}{3}\alpha a_1 + \frac{3}{4}r\right]\sin^2(\Theta) \quad (20)$$

$$F_\Theta = \mu_o(\lambda J_o)^2\left[-\frac{a_1^4}{6r^2} + \frac{2}{3}\alpha a_1 - \frac{1}{2}r\right]\sin(\Theta)\cos(\Theta) \quad (21)$$

The displacement vector $\vec{u}$ combines both tangential and radial displacements:[13]

$$\vec{u} = (u_r, u_\Theta, 0) \equiv (w, v, 0)$$

The displacements are related to the body force $\vec{F} = (F_r, F_\Theta, 0)$ by:

$$2(1-\nu)(\text{grad. div }\vec{u}) - (1-2\nu)(\text{rot rot }\vec{u}) = -2\vec{F}\,\frac{(1+\nu)(1-2\nu)}{E} \quad (22)$$

From these equations, we have calculated stresses and strains.[14] Some results of these calculations are used in Table IV, where are compared inductive storage coils.

Evaluation of stresses in <u>toroidal</u> coils is equally complex as for <u>spheres</u>, if we consider the nonuniform field distribution within the toroid, shown in Table III. Only for small values of $\alpha = r_1/R_o$, the assumption of a uniform field distribution may give a first order approximation to the stress-calculations. Taking the maximum value of B at point P, we may write for the hoop stresses:

$$\sigma_\Theta = r_1 B_{max}(\lambda J_o)\frac{\beta}{\beta-\alpha}\;\frac{2-\beta}{2(1-\beta)} \quad (23)$$

and for radial stresses:

$$\sigma_r = r_1 B_{max}(\lambda J_o)\frac{\beta}{2(\beta-\alpha)} \quad (24)$$

VI. Comparison of Inductive Energy Storage Coils

For an arbitrary selection of two energy levels 10^{10} J and 10^{13} J, we have calculated three types of inductive storage coils. The economical comparison may be based on Q_{SC}. The amount of superconductor depends primarily on the permissible stress limit. Since all equations relating the stored energy, the stresses and Q_{SC} are connected through the parameters α and β, by selecting a central field, a stress limit pertinent to the conductor and the energy to be stored, the calculation of Q_{SC} is fairly simple. For stainless steel reinforced Nb_3Sn tapes which was chosen as conductor we have limited the maximum hoop stress to less than 3500 $kpcm^{-2}$.

This limit does present somewhat of a problem, since the coil may be distorted. However, since the overall current density in the coils is in the order of 10^3 Acm^{-2}. less than 10% of the coil will be superconducting. The composite conductor can be reinforced by means of stainless steel tapes, or the superconductor can be embedded in a stainless steel or beryllium copper matrix.

In Table IV, three types of energy storage systems are compared. Looking at the spherical storage coil including a field screening coil, the total Q_{SC} is comparable to the amount of superconductor used in the toroidal coil. The Brooks coil seems to require less superconductor in the main coil, if we ignore the screen. However, if the field screening coil is provided, the difference in Q_{SC} for the three coils is not significant.

VII. Design Considerations

a) Static and Dynamic Losses

Energy storage coils have not only appreciable weight, but also a large external surface even if the bore is cold. Heat inleak occurs through the support structure into the coil by convection and through heat radiation from the external surface. The heat leak may be reduced by appropriate shaping of the coil support and the use of modern superinsulation as well as intermediate temperature heat

TABLE IV. Comparison between Inductive Energy Storage Coils

Basic Parameters:			
E_{tot}	(J)	10^{10}	10^{13}
$B_{o,o,o}$	(T)	10	10
Brooks Coil			
a_1	(m)	2.44	24.4
λJ_o	$(A\ m^{-2})$	$9.5x10^6$	$0.95x10^6$
$Q_{SC,coil}$	(A m)	$1.3x10^9$	$1.3x10^{11}$
σ_Θ	$(kp\ m^{-2})$	$3.2x10^7$	$3.2x10^7$
Thick Wall Spere			
a_1	(m)	2.36	23.6
α		1.6	1.6
λJ_o	$(A\ m^{-2})$	$1.1x10^7$	$1.1x10^6$
$Q_{SC,coil}$	(A m)	$1.5x10^9$	$1.5x10^{11}$
$\sigma_{\Theta,max}$	$(kp\ m^{-2})$	$\approx 3.3x10^7$	$\approx 3.3x10^7$
$Q_{SC,screen}$	(A m)	$\approx 1.4x10^9$	$\approx 1.4x10^{11}$
Toroidal Coil			
R_o	(m)	6.4	64
r_1	(m)	0.96	9.6
r_2	(m)	1.79	17.9
λJ_o	$(A\ m^{-2})$	$1.1x10^7$	$1.1x10^6$
Q_{SC}	(A m)	$3.1x10^9$	$3.1x10^{11}$
$\sigma_{\Theta,max}$	$(kp\ m^{-2})$	$\approx 3.4x10^7$	$\approx 3.4x10^7$
$\sigma_{r,max}$	$(kp\ m^{-2})$	$\approx 1.4x10^7$	$\approx 1.4x10^7$

shields between 4 K and 300 K which are familiar engineering problems. If energy is to be stored in large units over longer time periods a refrigerator replenishing the coolant is necessary. Time varying fields during the charge and discharge of energy result in losses in the superconductor. Losses in superconducting coils, when exposed to time varying magnetic fields have the following origins:[15,16]

Eddy current losses in the conductor matrix,

self field losses,

hysteretic losses,

losses due to mechanical movements,

auxiliary losses due to nonuniform magnetic fields over the coil,

hysteretic losses and losses due to conductor motion have the largest contribution, specifically since in high strength conductors twisting of fine superconducting filaments with small twist pitches may produce problems and cables do not have the equivalent strength of solid multifilamentary conductors used for dc applications.

If superconducting tapes are wound in coils, dissipative losses are enhanced considerably compared to multifilamentary conductors, as the field is not always parallel to the tape surface over the length of the conductor.

b) Coil Protection

Even if we eliminate any possibility of an accidental flux-perturbation or quench, provisions have to be made for rapid magnet discharge in the event of a transition from superconducting to a normal state. The transition may occur from loss of refrigeration, power breakdown, conductor material fatigue etc. Rapid discharge should be provided in order to prevent internal overheating, voltage breakdown and insulation damage.

Coil quench detection and protection devices with external watercooled shunts, rapidly operating high voltage switches and helium recovery systems are developed for large magnet systems.[17] With these devices available and the very low current densities chosen coil quenching should not present a serious problem.

c) Basic Economics

The cost of the superconducting energy storage system is given by the sum of the following items:

i) The cost of the coil.
ii) The cost of the cryostat and the refrigeration system.
iii) The cost of the switches and charging power supply.

The cost of the coil is a function of Q_{SC}, the winding preparation (fixtures, winding tables etc.) and the winding. Since the amount of superconductor used in the conductor is small, the conductor price will be moderate. To keep the cost of the coil low, simple coil geometries should be selected, as shown above. A major part of the cost will be in the reinforcement of the coils.

The cost of the cryostat and the refrigeration system is roughly proportional to the cryostat surface area. Since the coil bore is not used, it can be closed and evacuated such that heat inleaks occur only from the outer surface and the coil supports. The cryostat must also conform to the pressure code norms such that it withstands internal and external pressures in case of an accidental quench .

The power supply for charging an inductive energy storage system is a significant factor in the overall cost of the magnet, whereas it is quite small in the case of capacitors. Only if the coil can be charged quite slowly and discharged rapidly, the cost of the power supply may drop considerably.

The unknown factor in the overall cost estimate is the price of the superconducting switch. Although the design and manufacturing of coils is technically feasible in the sizes discussed there is no superconducting switch available, which is able to open circuits releasing 10^{10} J or more into loads in reasonable times. In this area, substantial development work is indicated.

VIII. Conclusions

Several geometric forms of energy storage systems have been considered. For energies above 10^7 J, superconducting coils are superior to electrical machines and batteries at discharge times of a few milliseconds to a few seconds. Thus, their usefulness is uncontested for the use in combination with fusion reactors. For slow energy discharge (> 10 sec), electrical machines and for very long discharge times, batteries appear to be much better suited and more economical than inductive storage units.

Present-day technology indicates that electromagnetic forces, dynamic losses, energy dissipation problems can be handled adequately. Combination of inductance and capacitors to extract all the energy from the storage unit is feasible; it should be checked if it is economically more attractive than inductances alone, even with their poor efficiency. In the major area of switching, only preliminary tests have been performed and energies in the order of ∿ 50 kJ are discharged into resistors and inductive coils. From practical point of view much higher currents are needed. Paralleling individual wires may yield desired result without conductor degradation.

As very high energies are needed in controlled thermonuclear reactors, the economics of fusion power will be influenced by the development of superconducting energy storage systems.

References

1. R. Carruthers, Culham Laboratory Report No. CLM-P7 (1961).
2. P.F. Smith and J.D. Lewin, Part. Acc. Vol. 1, 155 (1970).
3. M.S. Lubell et al., ORNL-TM-3927 (1972).
4. P. Komarek, Proc. 6th Symp. Fusion Techn., Aachen, EUR 4593e, 1970.
5. M.S. Lubell, Private Communication to S. Wipf.
6. O.K. Mawardi, U.S. Patent No. 3, 384, 762.
7. R.R. Hake, Los Alamos Report LA-4617-MS (1971).
8. H.L. Laquer, D.M. Weldon and F.L. Ribe, Los Alamos Report LA-DC-12228 (1971).
9. H. Brechna, Bulletin SEV No. 20, 910 (1967).
10. A. Malandain, Brown Boveri Mittlg. 1-1971.
11. A.J. Middleton and C.W. Trowbridge, Proc. Int. Conf. on Magnet Techn., 140, (1967).
12. A.D. Appleton, T.P. Cowhig and J. Caldwell, Proc. Int. Conf. on Magnet Techn., 553, (1967).
13. L.D. Landau, E.M. Lifschitz, Lehrbuch der Theoretischen Physik, Band VII, Berlin, Akad. Verl. 1965, p. 20.
14. H. Brechna and F. Arendt, KFK Report 1694 (1972).
15. G. Ries and H. Brechna, KFK Report 1372 (1972).
16. M.N. Wilson, Rutherford HEL Report RPP/A89 (1972).
17. F. Wittgenstein, Rev. Ind. Atomique No. 5/6, 23 (1970).